MOLECULAR PHYSICS REPORTS **40** (2004) 200-205

FIRST-PRINCIPLES STUDY OF MAGNETIZATION RELAXATION ENHANCEMENT IN THIN MAGNETIC FILMS

M. ZWIERZYCKI[1,2], Y. TSERKOVNYAK[3], P. J. KELLY[1], A. BRATAAS[4], AND G. E. W. BAUER[5]

[1]*University of Twente, Enschede, The Netherlands*
[2]*Institute of Molecular Physics, Polish Academy of Sciences, Poznań, Poland*
[3]*Harvard University, Cambridge, USA*
[4]*Norwegian University of Science and Technology, Trondheim, Norway*
[5]*Delft University of Technology, The Netherlands*

Abstract: The interface-induced magnetization damping of thin ferromagnetic films in contact with normal-metal layers is calculated from first principles for clean and disordered Fe/Au interfaces. Interference effects arising from coherent scattering turn out to be very small, consistent with a very small magnetic coherence length. Because the mixing conductances which govern the spin transfer are to a good approximation real valued, the spin pumping can be described by an increased Gilbert damping factor but an unmodified gyromagnetic ratio.

1. INTRODUCTION

The local magnetization dynamics in a bulk ferromagnet is usually well described by a phenomenological Landau-Lifshitz-Gilbert (LLG) equation [1]:

$$\frac{d\mathbf{m}}{dt} = -\gamma \mathbf{m} \times \mathbf{H}_{\text{eff}} + \alpha \mathbf{m} \times \frac{d\mathbf{m}}{dt}, \tag{1}$$

where $\mathbf{m}$ is the magnetization-direction unit vector, $\mathbf{H}_{\text{eff}}$ an effective magnetic field and γ a gyromagnetic ratio. The Gilbert-damping constant α parametrizes the viscous damping of an- excited magnetization to the (locally) lowest-energy configuration. A considerable enhancement (in comparison to the bulk values) of the Gilbert-damping coefficient has been observed in FMR experiments for the ultra-thin magnetic layers [2-5]. This enhancement can be explained in terms of the spin-pumping effect: a time-dependent ferromagnetic order parameter pumps spin currents that carry angular momentum (and energy) into adjacent conducting materials [6, 7]. The angular-momentum loss, in turn, is equivalent to an additional damping torque on the magnetization. Here we extend the previous phenomenological treatment [6, 7] with the first principles calculations which take into account the detailed atomic and electronic structure of the materials under study.

2. THEORY

Coherent motion of the magnetization, whose direction is given by the unit vector $\mathbf{m}(t)$, leads to the emission of a spin current [6, 7]

$$\mathbf{I}_s = \frac{\hbar}{4\pi}\left(\mathrm{Re}\, A^{\uparrow\downarrow}\mathbf{m}\times\frac{d\mathbf{m}}{\mathbf{dt}} + \mathrm{Im}\, A^{\uparrow\downarrow}\frac{d\mathbf{m}}{dt}\right) \tag{2}$$

per unit area of the contact into each normal-metal layer, which we will here assume is then fully absorbed by the neighbouring non-magnetic layers acting as perfect spin-sinks (reservoirs). The complex spin-pumping conductance $A^{\uparrow\downarrow} = g^r_{\uparrow\downarrow} - g^t_{\uparrow\downarrow}$ is the difference between the reflection ($g^r_{\uparrow\downarrow}$) and transmission ($g^t_{\uparrow\downarrow}$) mixing conductances (per contact unit area) defined in terms of the spin-dependent reflection and transmission coefficients of the ferromagnetic film as [6, 7]:

$$g^r_{\uparrow\downarrow} = S^{-1}\sum_{mn}\left(\delta_{mn} - r^{\uparrow}_{mn}r^{\downarrow *}_{mn}\right), \tag{3}$$

$$g^t_{\uparrow\downarrow} = S^{-1}\sum_{mn} t'^{\uparrow}_{mn}t'^{\downarrow *}_{mn}. \tag{4}$$

Here, S is the F/N contact area, m and n denote scattering states at the Fermi energy of the normal-metal leads. The total angular-momentum loss of the ferromagnet is given by a sum of contributions (2) from the two leads, characterized by two spin-pumping parameters $A_1^{\uparrow\downarrow}$ and $A_2^{\uparrow\downarrow}$. Adding this source of spin angular-momentum current to the right-hand side of Eq. (1) leads to a new LLG equation for the monodomain thin film with saturation magnetization M_s embedded in the non-magnetic conducting medium, with the modified constants α_{eff} and γ_{eff} [6],

$$\frac{1}{\gamma_{\mathrm{eff}}} = \frac{1}{\gamma}\left[1 - \frac{\hbar\gamma}{4\pi M_s d}\,\mathrm{Im}\left(\mathrm{A}_1^{\uparrow\downarrow} + \mathrm{A}_2^{\uparrow\downarrow}\right)\right], \tag{5}$$

$$\alpha_{\mathrm{eff}} = \frac{\gamma_{\mathrm{eff}}}{\gamma}\left[\alpha + \frac{\hbar\gamma}{4\pi M_s d}\,\mathrm{Re}\left(\mathrm{A}_1^{\uparrow\downarrow} + \mathrm{A}_2^{\uparrow\downarrow}\right)\right]. \tag{6}$$

The real part of $A^{\uparrow\downarrow}$ is always non-negative [6] so the correction to the damping is always positive. Anticipating the numerical results discussed later on, we note here that in typical situations $g^t_{\uparrow\downarrow}$ and $\mathrm{Im}\, g^r_{\uparrow\downarrow}$ (and thus $\mathrm{Im} A^{\uparrow\downarrow}$) are negligible so that the only effect of the spin pumping is to make an additional contribution to the Gilbert-damping parameter.

When the magnetic layer is embedded in the diffusive medium the "bare" conductance (3) has to be corrected for the corresponding "spurious" Sharvin (contact) resistance as discussed in Ref. 8. Additionally, a non-vanishing backflow and reabsorption of the emitted spins by the ferromagnet has to be taken into account (see Ref. 7). In the case of an $F/N/F$ structure (considered in Refs. 3-5) this leads to the effective mixing conductance [7]

$$\frac{1}{\widetilde{A}^{\uparrow\downarrow}_{F/N/F}} = 2\left(\frac{1}{g^r_{\uparrow\downarrow}} - \frac{1}{2g^{\mathrm{Sh}}_N} + \frac{e^2}{h}\frac{L}{\sigma}\right) \tag{7}$$

which enters Eqs. (5) and (6) instead of the sum $A_1^{\uparrow\downarrow} + A_2^{\uparrow\downarrow}$. Equation (7) is valid for the globally diffuse system with the well separated individual ferromagnetic resonances and only weakly excited from collinear configuration. Here g_N^{Sh} is the Sharvin conductance (given by the number of the propagating modes at the Fermi energy) of the normal-metal layer with thickness L and conductivity (per spin) $\sigma/2$. The factor 2 in Eq. (7) corresponds to the fact that the spin accumulation in the normal layer leads to a backflow of spins which splits equally between the two magnetic layers.

The effect of spin-dependent scattering on the time evolution of the magnetic order parameter is therefore mostly governed by three parameters: the reflection and transmission mixing conductances of the ferromagnetic layer, $g_{\uparrow\downarrow}^r$ and $g_{\uparrow\downarrow}^t$, and the Sharvin conductance of the normal metal, g_N^{Sh}. These quantities are accessible to *ab initio* band-structure calculations [9]. In the following we demonstrate this for Au/Fe(001) system routinely used by the Simon-Fraser group [3-5].

3. FIRST-PRINCIPLES METHOD

Parameter-free calculations of transmission and reflection coefficients were performed using the local-density approximation (LDA) of density-functional theory (DFT) in a two-step procedure. In the first step, the self-consistent electronic structure (spin densities and potentials) of the system was determined using the layer TB-LMTO (tight-binding linear muffin-tin orbital) surface Green's function (SGF) method in the atomic-sphere approximation (ASA) [10]. The atomic-sphere (AS) potentials of 4 monolayers on either side of the magnetic layer (or interface) were iterated to self-consistency while the potentials of more distant layers were held fixed at their bulk values. The common lattice constants was assumed for both metals of a structure: $a_{\mathrm{Au/Fe}} = \sqrt{2} \times 2.866 = 4.053$ Å. In the second step, the AS potentials serve as inputs to calculate scattering coefficients using a recently-developed scheme based on TB-MTOs [9]. Disorder is modelled using repeated lateral 10×10 supercells. The two-dimensional Brilloun zone (2D BZ) summation was performed using $k_{\|}$-mesh densities equivalent to 10^4 points in a 2D BZ of a 1×1 interface unit cell.

4. RESULTS AND DISCUSSION

Figure 1 shows how $G_{\uparrow\downarrow}^r = \left(e^2 / h\right) g_{\uparrow\downarrow}^r$ and $G_{\uparrow\downarrow}^t = \left(e^2 / h\right) g_{\uparrow\downarrow}^t$ depend on the thickness d of the magnetic layer (measured in atomic layers) for specular ($k_{\|}$-preserving) Au/Fe/Au (001) system. The quasi-oscillatory behaviour exhibited by both quantities arises from the phases accumulated by electrons on their passage through the magnetic layer (quantum size effect). These phases differ significantly between majority- and minority-spin states and are further modified (independently in each spin channel) by the matching of the states at the *F*/*N* interfaces. Consequently the $r^{\uparrow} r^{\downarrow *}$ and $t^{\uparrow} t^{\downarrow *}$ products in Eqs. (3) and (4) remain complex-valued (*i.e.* the phases do not cancel out) and vary in the complex plane as the function of $k_{\|}$. This leads to the cancellation in course of the integration over 2D BZ and the fast damping of the oscillations visible especially for $G_{\uparrow\downarrow}^t$.

Figure 2 shows the same quantities ($G^r_{\uparrow\downarrow}$ and $G^t_{\uparrow\downarrow}$) calculated for Au/Fe/Au(001) system in the presence of disorder modelled by 1 monolayer of 50% alloy added on each side of the magnetic layer. The effect of disorder is to strongly reduce the amplitudes of the (quasi)-oscillations. The reflection mixing conductance becomes practically constant at the level of its asymptotic (*i.e.* interfacial) value. For $G^t_{\uparrow\downarrow}$, the oscillations are not entirely damped out but their amplitude is substantially reduced. In fact, the values of $G^t_{\uparrow\downarrow}$ become negligible compared to $\mathrm{Re}\, G^r_{\uparrow\downarrow}$ for all but the thinnest magnetic layers. In addition, we expect that diffusive scattering in the bulk of the magnetic layer, which for simplicity has not been included here, will have a similar effect.

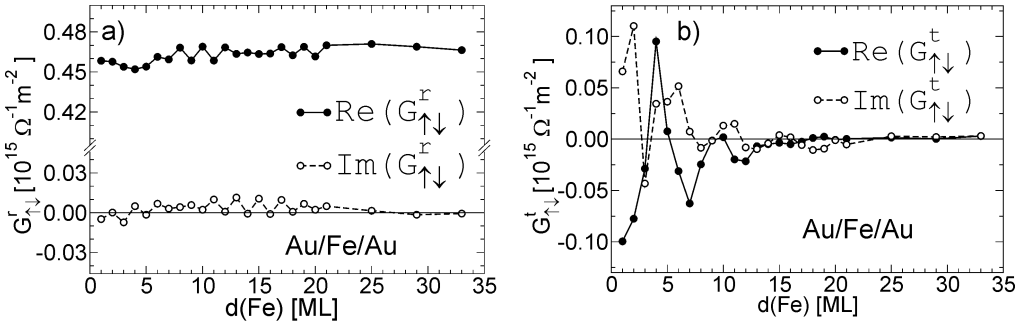

Fig. 1. Reflection (a) and transmission (b) spin-mixing conductance (per unit area) of a Au/Fe/Au(001) trilayer with perfect interfaces as a function of the thickness d of the Fe layer. In this and subsequent plots, mixing conductances expressed in terms of number of conduction channels per unit area are converted to $\Omega^{-1}\mathrm{m}^{-2}$ using the conductance quantum e^2/h, *i.e.* $G_{\uparrow\downarrow} = (e^2/h)g_{\uparrow\downarrow}$

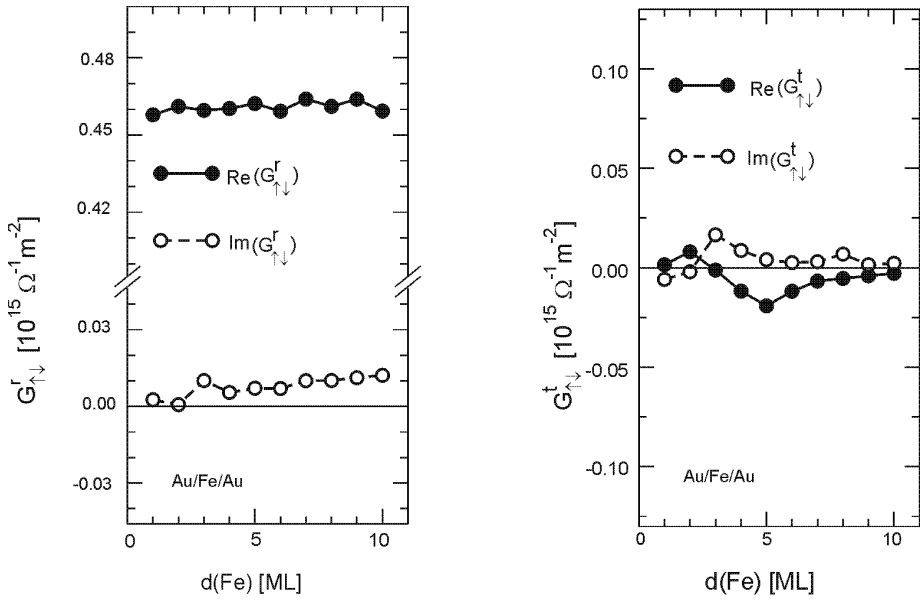

Fig. 2. Spin-mixing conductances of a Au/Fe/Au(001) trilayer with disordered interfaces as a function of the thickness d of the Fe layer

In view of the above results, we conclude that in a typical situation $A^{\uparrow\downarrow} \approx g^r_{\uparrow\downarrow}$, where $g^r_{\uparrow\downarrow}$ can be taken at its asymptotic value or calculated simply for an *N*/*F* interface instead of a complete structure. Qualitatively similar results have been obtained for the Cu/Co(111) system not discussed here.

In Ref. 3, Urban *et al*. reported room-temperature (RT) observations of increased Gilbert damping for a system consisting of two Fe layers separated by a Au spacer layer. The magnetization of the thinner of the to ferromagnetic layers precesses in the external magnetic field. The other ferromagnetic layer, with the direction of its magnetization fixed, acts as a spin sink. In the presence of a second Fe layer, Eq. (7) should be used. Neglecting Im $\tilde{A}_{F/N/F}$ leads to $\gamma_{\text{eff}} = \gamma$ and the damping enhancement

$$\alpha_{\text{eff}} - \alpha = \frac{\gamma \,\mathrm{Re}\, \tilde{A}_{F/N/F}}{4\pi M_s d}, \tag{8}$$

where $\alpha \approx 0.004$ is the damping measured for a single layer. Using [11] $\gamma = 2.1\ \mu_B/\hbar$ the asymptotic value of $\mathrm{Re}(G^t_{\uparrow\downarrow})$ from Figs. 1, 2 and the Sharvin conductance of Au: $0.46 \times 10^{15}\Omega^{-1}$ m^{-2}, Eq. (8) is compared with the experimental data in Fig. 3 for various assumptions about σ in (7). In the low temperature limit and neglecting the residual resistivity of the Au layer, $\sigma \to \infty$, Eq. (8) yields the solid line which is seen to overestimate the damping enhancement compared to the measured results. Using finite values of σ will lead to lower values of $\tilde{A}$ and indeed, it was found experimentally [4] that lowering the temperature (increasing the conductivity) increases the damping by as much as about 20% (open circle in Fig. 3). If we use the room temperature (RT) conductivity due to phonon scattering in crystalline bulk Au [12], $\sigma_{ph} = 0.45 \times 10^8\ \Omega^{-1}$ m^{-1}, the dashed line is obtained which, as expected, is closer to the RT measurements. Measurements of the sheet conductivity [4] indicate that the Au layers used in the experiments have non-negligible residual resistances. Assuming a value of $\sigma_{res} = 0.24 \times 10^8\ \Omega^{-1}$ m^{-1}, we can obtain quite close agreement between theory and experiment as shown by the corresponding 0 K (chain line) and RT (dotted line) curves in Fig. 3. The RT line is obtained assuming that phonon and defect scattering contribute to the resistance additively (Matthiessen's rule).

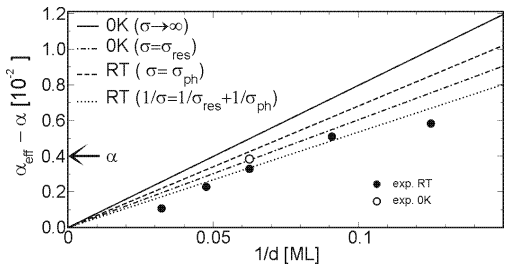

Fig. 3. Enhancement of the Gilbert damping coefficient for an Fe/Au/Fe trilayer as a function of 1/*d* where *d* is the thickness of the Fe layer. The filled circles (●) are the RT values measured in Ref. 3 and the open one (○) is a low temperature value from Ref. 4. The theoretical predictions based on Eq. (8) for 0 K are shown as solid (with $\sigma \to \infty$) and chain (with residual resistivity) lines, the RT-corrected ones as dashed (with phonon scattering) and dotted (phonon and defect scattering) lines. The value of the Gilbert damping α for a single Fe film is marked with an arrow

In conclusion we have demonstrated that direct first-principles calculations can produce values of the damping coefficient in the same range as those measured experimentally. What is more, by taking into account various other sources of scattering in the Au spacer and/or quantum-size effects, the calculations can be brought into very close agreement with experiment. A more definitive quantitative comparison with experiment would require a detailed knowledge of the microscopic structure of the experimental system which is currently not available.

The reorientation of the magnetization of one or more of the magnetic layers in the multilayer is the typical mode of operation of the magnetoelectronic devices. Understanding the dynamics of this process and possibly its optimization (*e.g.* by engineering the system with required damping characteristics) is therefore a thing of both fundamental and practical importance.

References

[1] T. L. Gilbert, Phys. Rev. **100**, 1243 (1955); L. D. Landau, E. M. Lifshitz, and L. P. Pitaevski, *Statistical Physics*, *part 2*, Pergamon, Oxford 1980, (3rd ed).
[2] S. Mizukami, Y. Ando, and T. Miyazaki, Jpn. J. Appl. Phys. **20**, 580 (2001); J. Magn. Magn. Mater. **226**, 1640 (2001).
[3] R. Urban, G. Woltersdorf, and B. Heinrich, Phys. Rev. Lett. **87**, 217204 (2001).
[4] B. Heinrich, G. Woltersdorf, R. Urban, and E. Šimánek, J. Appl. Phys. **93**, 7545 (2003).
[5] B. Heinrich, Y. Tserkovnyak, G. Woltersdorf, A. Brataas, R. Urban, and G. E. W. Bauer, Phys. Rev. Lett. **90**, 187601 (2003).
[6] Y. Tserkovnyak, A. Brataas, and G. E. W. Bauer, Phys. Rev. Lett. **88**, 117601 (2002).
[7] Y. Tserkovnyak, A. Brataas, and G. E. W. Bauer, Phys. Rev. **B66**, 224403 (2002).
[8] G. E. W. Bauer, Y. Tserkovnyak, D. Huertas-Hernando, and A. Brataas, Phys. Rev. **B67**, 094421 (2003).
[9] K. Xia, P. J. Kelly, G. E. W. Bauer, I. Turek, J. Kudrnovský, and V. Drchal, Phys. Rev. **B63**, 094421 (2001).
[10] I. Turek, V. Drchal, J. Kudrnovský, M. Šob, and P. Weinberger, *Electronic Structure of Disordered Alloys, Surfaces and Interfaces*, Kluwer, Boston-London-Dordrecht 1997; O. K. Andersen, O. Jepsen, and D. Glötzel, in: *Highlights in Condensed Matter Theory*, ed. F. Bassani, F. Fumi, and M. P. Tosi, North-Holland, Amsterdam 1985: 59.
[11] B. Heinrich, K. B. Urquhart, A. S. Arrott, J. F. Cochran, K. Myrtle, and S. T. Purcell, Phys. Rev. Lett. **59**, 1756 (1987).
[12] http://www.webelements.com/